

# Medium effect in high density region probed by nucleus-nucleus elastic scattering

T. Furumoto\*

*National Institute of Technology, Ichinoseki College, Ichinoseki, Iwate 021-8511, Japan*

Y. Sakuragi

*Department of Physics, Osaka City University, Osaka 558-8585, Japan*

Y. Yamamoto

*RIKEN Nishina Center, RIKEN, Wako, Saitama 351-0198, Japan*

(Dated: January 31, 2019)

## Abstract

We investigate the sensitivity of the medium effect in the high density region on the nucleus-nucleus elastic scattering in the framework of the double-folding (DF) model with the complex  $G$ -matrix interaction. First, the evaluating position of the local density, which is an ambiguity of the DF model, is investigated. However, the effect has a minor role to the  $^{16}\text{O} + ^{16}\text{O}$  system. Next, the medium effect including three-body-force (TBF) effect is investigated with two methods. In the both methods, the medium effect is clearly seen on the potential and the elastic cross section, but not on the total reaction cross section. Finally, we make clear the crucial role of the TBF effect up to  $k_F = 1.6 \text{ fm}^{-1}$  in the nucleus-nucleus elastic scattering.

PACS numbers: 21.30.-x, 24.10.-i, 24.10.Ht, 25.70.Bc

---

\*Electronic address: furumoto@ichinoseki.ac.jp

## I. INTRODUCTION

The optical model potential (OMP) is one of key issues for the nuclear physics not only to analyze the nuclear reaction data but also to understand nuclear reaction mechanism. Historically, the OMP is constructed from the phenomenological way to reproduce the experimental elastic scattering data. It is indispensable to reproduce the experimental elastic scattering data for the OMP so as to apply it to the several nuclear reaction models (Distorted Wave Born Approximation model and Coupled-Channel model and so on). However, the phenomenological OMP has a large ambiguity for the inner part of the potential. Namely, the phenomenological OMP can reproduce the data but one is not always unique. Then, the more reliable method to construct the OMP is required. In order to solve the problem, the folding model is proposed. The model is the simplest but powerful tool to construct the nucleus-nucleus (or nucleon-nucleus) potential by folding the densities of the colliding two (or one) nuclei with the nucleon-nucleon ( $NN$ ) interaction. For the nucleus-nucleus system, the density-independent  $NN$  interaction (M3Y) is applied to the double-folding (DF) model in the embryonic stage [1, 2]. Thereafter, the reliability of the DF potential has been consolidated by proposing the phenomenological density-dependent  $NN$  interactions [3–7]. Then, the analyses of the nuclear reaction data is advanced with the DF model. However, those phenomenological density-dependent  $NN$  interactions have no imaginary part. Consequently, the imaginary part of the OMP is still constructed by phenomenological way.

To construct not only the real part but also the imaginary part from the microscopic view point, the complex  $G$ -matrix interactions have been applied to the DF model [8–12]. Those complex  $G$ -matrix interactions are successful to describe the nucleon-nucleus scattering in the framework of the single-folding model. The application to nucleus-nucleus system seems like working well and the various experimental data are analyzed. However, the success of the complex potential is limited, and it is suggested that the existing complex  $G$ -matrix interactions lack the information in the high density region (up to twice the normal density) for the nucleus-nucleus system in Ref. [12]. The prescription of the local density in the DF model is not suitable for example the local density is treated as arithmetic-geometric mean in the case with the JLM interaction. In the DF model, the folded densities are not broken through the nuclear reaction even if colliding two nuclei close to each other. Then, the frozen density approximation (FDA), which is assumed as keeping the form and strength of the

density in the nuclear reaction, is considered as the most suitable prescription in the DF model and the effect and justification are discussed in Refs. [12–14]. In the situation, the complex  $G$ -matrix interaction is needed up to twice the normal density because the local density reaches up to twice the normal density by FDA.

Recently, the authors propose the complex  $G$ -matrix interaction, CEG07 [14, 15], whose density dependence is calculated up to twice the normal density ( $k_F = 1.8 \text{ fm}^{-1}$ ). Then, they have applied the CEG07 interaction to the DF model, and the DF potential with the CEG07 interaction well reproduces the experimental data of the nucleus-nucleus elastic scattering [14, 16, 17]. The reliable complex optical potential between colliding nuclei is constructed from the microscopic view point. In Refs. [14, 16], it is made clear that the three-body-forces (TBFs) effect, especially the repulsive component of the TBF effect, plays an important role to reproduce the precise angular distribution of the nucleus-nucleus scattering up to backward angles while the TBF effect is introduced phenomenologically. In Refs. [14–16], the three-body repulsive effect was represented conveniently by changing masses of exchanged vector mesons in nuclear medium. In Ref. [18], the similar effect was given more clearly as a multi-pomeron exchange potential (MPP). The strengths of MPP were determined by the analysis of the  $^{16}\text{O} + ^{16}\text{O}$  elastic scattering with the DF potential from complex  $G$ -matrix interactions in the same way as the present work. The MPP model includes triple and quartic pomeron exchanges, and can lead to the neutron-star EOS stiff enough to reproduce a maximum star mass over  $2M_{\text{soler}}$ . Recently, such a conclusion has been obtained even in hyperon-mixed neutron-star matter [19]. Thus, our DF model analyses based on FDA are demonstrated to be quite useful to find many-body repulsive effects in high density EOS, for which high-energy central heavy-ion collisions or any other experiments still remain inconclusive. One of purposes in this work is to make clear the reason why our DF model analyses are so useful to obtain valuable information in the high-density region.

In this paper, we apply the complex  $G$ -matrix interaction based on the ESC08 interaction with the MPP model [18–21] to the DF model calculation. The density distribution of the light nucleus is almost formed by the nuclear surface. The density rapidly decreases from the saturation density to 0 in the nuclear surface region. The effect gives the large ambiguity of the evaluating position of the local density. Then, we first investigate the ambiguity of the evaluating position of the local density. In the DF model, it is considered that the local density through the FDA reaches up to about the twice the normal density. Next, the

detail of the medium effect in the high density region is unknown in the DF potential and the observation for the nucleus-nucleus system. In this paper, we investigate the role and sensitivity of the medium effect including the TBF effect in the high density region by the DF model with the complex  $G$ -matrix interaction. Finally, we make clear that the important role of medium effect including the TBF effect in high density region on the heavy-ion elastic scattering.

## II. FORMALISM

We construct the nucleus-nucleus potential based on the DF model with the use of the complex  $G$ -matrix interaction including the TBF effect based on the MPP model. The microscopic nucleus-nucleus potential can be written as a Hartree-Fock type potential;

$$U = \sum_{i \in A_1, j \in A_2} [\langle ij | v_D | ij \rangle + \langle ij | v_{\text{EX}} | ji \rangle] \quad (1)$$

$$= U_D + U_{\text{EX}}, \quad (2)$$

where  $v_D$  and  $v_{\text{EX}}$  are the direct and exchange parts of complex  $G$ -matrix interaction. The exchange part is a nonlocal potential in general. However, by the plane-wave representation for the  $NN$  relative motion [22, 23], the exchange part can be localized. The direct and exchange parts of the localized potential are then written in the standard form of the DF potential as

$$U_D(R) = \int \rho_1(\mathbf{r}_1) \rho_2(\mathbf{r}_2) v_D(s; \rho, E/A) d\mathbf{r}_1 d\mathbf{r}_2, \quad (3)$$

where  $\mathbf{s} = \mathbf{r}_2 - \mathbf{r}_1 + \mathbf{R}$ , and

$$U_{\text{EX}}(R) = \int \rho_1(\mathbf{r}_1, \mathbf{r}_1 + \mathbf{s}) \rho_2(\mathbf{r}_2, \mathbf{r}_2 - \mathbf{s}) v_{\text{EX}}(s; \rho, E/A) \\ \times \exp \left[ \frac{i\mathbf{k}(R) \cdot \mathbf{s}}{M} \right] d\mathbf{r}_1 d\mathbf{r}_2. \quad (4)$$

Here,  $\mathbf{k}(R)$  is the local momentum for nucleus-nucleus relative motion defined by

$$k^2(R) = \frac{2mM}{\hbar^2} \{E_{\text{c.m.}} - \text{Re } U(R) - V_{\text{Coul.}}(R)\}, \quad (5)$$

where  $M = A_1 A_2 / (A_1 + A_2)$ ,  $E_{\text{c.m.}}$  is the center-of-mass energy,  $E/A$  is the incident energy per nucleon,  $m$  is the nucleon mass and  $V_{\text{Coul.}}$  is the Coulomb potential.  $A_1$  and  $A_2$  are the mass numbers of the projectile and target, respectively. The exchange part is calculated

self-consistently on the basis of the local energy approximation through Eq. (5). Here, the Coulomb potential  $V_{\text{coul}}$  is also obtained by folding the  $NN$  Coulomb potential with the proton density distributions of the projectile and target nuclei. The density matrix  $\rho(\mathbf{r}, \mathbf{r}')$  is approximated in the same manner as in [24];

$$\rho(\mathbf{r}, \mathbf{r}') = \frac{3}{k_F^{\text{eff}} \cdot s} j_1(k_F^{\text{eff}} \cdot s) \rho\left(\frac{\mathbf{r} + \mathbf{r}'}{2}\right), \quad (6)$$

where  $k_F^{\text{eff}}$  is the effective Fermi momentum [25] defined by

$$k_F^{\text{eff}} = \left\{ \left( \frac{3\pi^2}{2} \rho \right)^{2/3} + \frac{5C_s(\nabla\rho)^2}{3\rho^2} + \frac{5\nabla^2\rho}{36\rho} \right\}^{1/2}, \quad (7)$$

where we adopt  $C_s = 1/4$  following Ref. [26]. The exponential function in Eq. (4) is approximated by the leading term of the multipole expansion, namely the spherical Bessel function of rank 0,  $j_0(\frac{k(R)s}{M})$ , following the standard prescription [15, 27–31].

In the present calculations, we employ the FDA for the local density as mentioned in introduction. In the FDA, the density-dependent  $NN$  interaction is assumed to feel the local density defined as the sum of densities of colliding nuclei evaluated;

$$\rho = \rho_1 + \rho_2. \quad (8)$$

The FDA has been widely used also in the standard DF model calculations [2, 5, 7, 26, 32]. In Ref. [14], it is confirmed that FDA is the best prescription in the case with complex  $G$ -matrix interaction to reproduce the data.

### III. RESULTS

We now apply the complex  $G$ -matrix interactions, which is constructed from the ESC08 interaction with the MPP model [18, 20, 21], to nucleus-nucleus systems through the DF model. There have been proposed three versions of the MPP model (MPa/b/c) [19], which reproduce the  $^{16}\text{O} + ^{16}\text{O}$  angular distribution equally well but give rise to different stiffness of EOS. We use here the MPa version giving the stiffest EOS. In this paper, we investigate the medium effect for the elastic scattering of the  $^{16}\text{O} + ^{16}\text{O}$  system at  $E/A = 70$  MeV the same as in the Refs. [14, 16]. We adopt the nucleon density of the  $^{16}\text{O}$  nucleus calculated from the internal wave functions generated by the orthogonal condition model (OCM) by Okabe [33] based on the microscopic  $\alpha + ^{12}\text{C}$  cluster picture.

### A. Evaluating position of local density

First, we investigate the sensitivity of the DF model potential and the scattering cross section to the evaluating position of the local density in order to reveal the ambiguity in the local density approximation. To this end, we compare the results with the two types of prescriptions to evaluate the local density, defined as,

$$\rho_{\text{mid.}} = \rho_1(\mathbf{r}_1 + \frac{1}{2}\mathbf{s}) + \rho_2(\mathbf{r}_2 - \frac{1}{2}\mathbf{s}), \quad (9)$$

$$\rho_{\text{each}} = \rho_1(\mathbf{r}_1) + \rho_2(\mathbf{r}_2). \quad (10)$$

In the  $\rho_{\text{mid.}}$  prescription, the local density is evaluated at the middle point of the interacting nucleon pair, and we call this prescription as "middle" in short. On the other hand, in the  $\rho_{\text{each}}$  prescription, the local density is evaluated at the positions of each nucleon, and we call this prescription as "each" in short. In Ref. [14], this prescription was applied only to direct part of the DF potential, while in the present paper it is applied both to the direct and exchange parts.

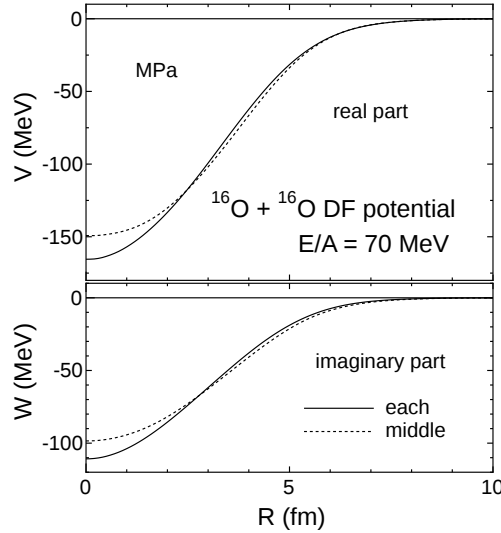


FIG. 1: The real and imaginary parts of the DF potential for the  $^{16}\text{O} + ^{16}\text{O}$  system at  $E/A = 70$  MeV. The solid and dotted curves are the results with the each and middle prescriptions, respectively.

Figure 1 shows the real (upper panel) and imaginary (lower panel) parts of the calculated DF potential for the  $^{16}\text{O} + ^{16}\text{O}$  elastic scattering at  $E/A = 70$  MeV with the use of two

prescriptions defined in Eqs. (9) and (10). The effect of the evaluating position of the local density is seen on the real and imaginary parts of the DF potential. The effect of the position of the local density is the same as each other on the real and imaginary parts of the DF potential. For the tail part, the DF potential by the middle prescription is more attractive than that by the each prescription because the complex  $G$ -matrix interaction for the middle prescription feels weaker medium effect (lower density) than that for the each prescription around the tail part. On the other hand, the inner part of the DF potential by the each prescription gives deeper potential than that by the middle prescription. For the inner part, the interaction by the each prescription feels weaker medium effect because the density is almost formed by the nucleus surface region for the light nucleus.

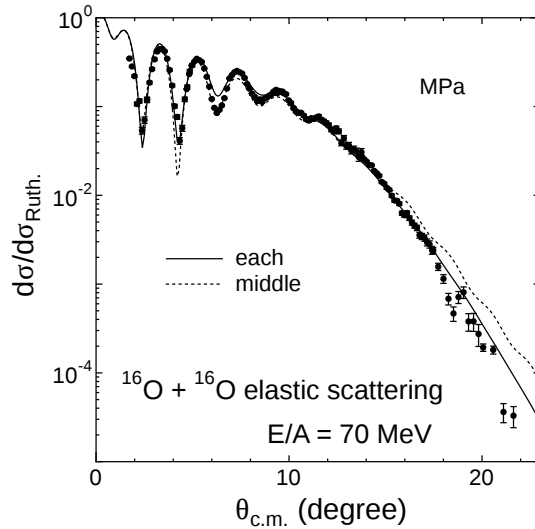


FIG. 2: Rutherford ratio of the cross sections for the  $^{16}\text{O} + ^{16}\text{O}$  elastic scattering at  $E/A = 70$  MeV. The meaning of the curves is the same as in Fig. 1. The experimental data is taken from Ref. [34].

TABLE I: The calculated total reaction cross section for the  $^{16}\text{O} + ^{16}\text{O}$  system at  $E/A = 70$  MeV.

middle (mb)	each (mb)
1503	1426

Figure 2 shows the results calculated with the DF potential shown in Fig. 1 for the  $^{16}\text{O} + ^{16}\text{O}$  elastic scattering at  $E/A = 70$  MeV. The minor effect of the evaluating position of the local density can be confirmed from Fig. 2. Note that no renormalization factor is

introduced here both to the real and imaginary parts of the calculated DF model potential to optimize the fit to the experimental data. However, we do not intend to emphasize the parameter free nature of the theoretical calculation with the present DF model. The absence of the adjustable parameter (renormalization factor) in reproducing the observed cross sections for the present scattering system,  $^{16}\text{O} + ^{16}\text{O}$ , is not essential in the discussion of the evaluating positions of local density or of the importance of the medium effect at high-density region (to be discussed in the following subsections). In fact, some renormalization of the imaginary part of the DF model potential is found to be necessary in other scattering systems, such as the  $^{12}\text{C} + ^{12}\text{C}$  one, in order to optimize the fit to the observed elastic cross sections, although the real part still needs not to be renormalized from the original strength of the theoretical DF model potential in all the scattering systems investigated so far.

In addition, we calculate the total reaction cross section for the  $^{16}\text{O} + ^{16}\text{O}$  system at  $E/A = 70$  MeV. The calculated results are shown in Table I. For the total reaction cross section, the difference between the calculated results of the each and middle prescriptions comes from the tail part of the DF potential.

## B. Medium effect in high-density region

Next, we investigate the medium effect for the high density region in the framework of the DF model with complex  $G$ -matrix interaction. We already mentioned the importance of the medium effect, especially the TBF effect, for the nucleus-nucleus elastic scattering in Refs. [14, 16]. However, the detail of the medium effect in the high-density region is not investigated. Then, we test the sensitivity of the medium effect in the high density region by the following artificial cut of the evaluated local density;

$$\rho = \begin{cases} \rho_1 + \rho_2 & \dots \text{ (if } \rho_1 + \rho_2 < \rho_{\text{cut}}) \\ \rho_{\text{cut}} & \dots \text{ (if } \rho_1 + \rho_2 > \rho_{\text{cut}}) \end{cases}, \quad (11)$$

by changing  $\rho_{\text{cut}}$  value as a parameter. In this paper, we calculate the DF potentials with several  $k_{\text{cut}}$  values where  $k_{\text{cut}}$  is defined by

$$\rho_{\text{cut}} = \frac{2}{3\pi^2} k_{\text{cut}}^3. \quad (12)$$

By changing the  $k_{\text{cut}}$  value, the medium effect in the high-density region is controlled and investigated in the potential and observable cross section.





In addition, we disclose the imperfection of the DF potential with the JLM [35], original CEG [30, 36], and Melbourne- $G$  [37] interactions, whose medium effect are calculated only up to  $k_F = 1.4 \text{ fm}^{-1}$ .

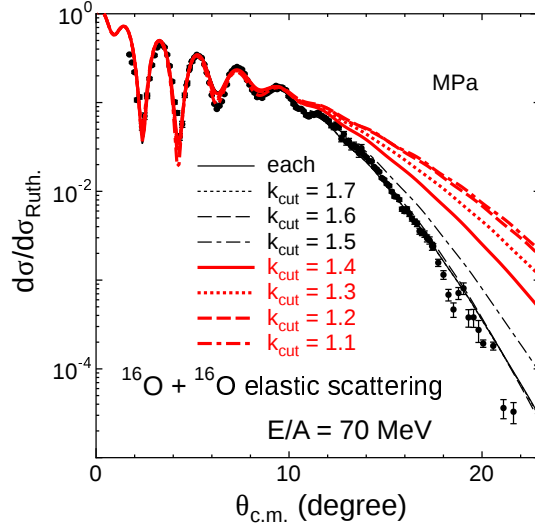


FIG. 4: (Color online) The elastic cross section with the DF potentials shown in Fig. 3. The meaning of the curves is the same as in Fig. 3.

Figure 4 shows the results calculated with the DF potentials shown in Fig. 3 for the  $^{16}\text{O} + ^{16}\text{O}$  elastic scattering at  $E/A = 70 \text{ MeV}$ . The medium effect is clearly seen up to  $k_F = 1.6 \text{ fm}^{-1}$  in the elastic cross section while the effect is seen up to  $k_F = 1.8 \text{ fm}^{-1}$  in the potential. The difference of the  $k_F$  values comes from the ambiguity of the inner part of the complex potential. In addition, we calculate the total reaction cross section with the DF potentials shown in Fig. 3. The calculated results are shown in Table II. The total reaction cross section almost has no sensitivity of the medium effect in the high density region. Namely, it is difficult to discuss the detail of the medium effect with the total reaction cross section.

Here, one might expect that the worse fits of the calculated cross sections with  $k_{\text{cut}} \leq 1.5 \text{ fm}^{-1}$  to the experimental data at large angles (shown in Fig. 4) could be recovered by the increase of absorption, namely by the introduction of the renormalization factor  $N_W > 1.0$  to the imaginary part of the calculated DF model potential with  $k_{\text{cut}} \leq 1.5 \text{ fm}^{-1}$ , as

$$U = V + iN_W W, \quad (13)$$

TABLE II: The calculated total reaction cross section for the  $^{16}\text{O} + ^{16}\text{O}$  system at  $E/A = 70$  MeV.

$k_{\text{cut}}$ ( $\text{fm}^{-1}$ )	Total reaction cross section (mb)
1.7	1426
1.6	1428
1.5	1429
1.4	1432
1.3	1441
1.2	1456
1.1	1476

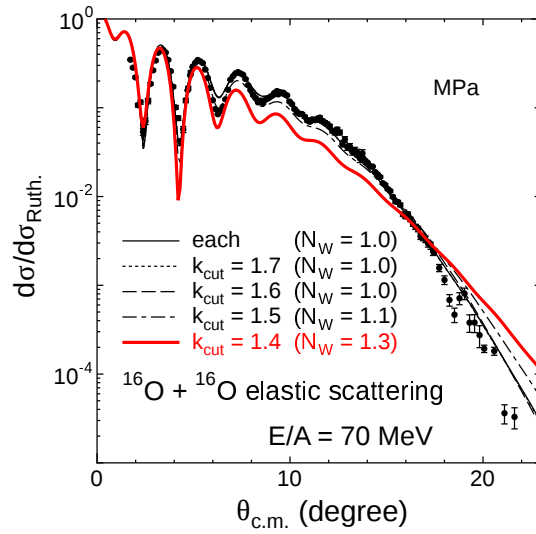


FIG. 5: (Color online) The elastic cross section with the DF potentials shown in Fig. 3 in the case with the renormalization factor,  $N_W$ , for the imaginary part. The meaning of the curves is the same as in Fig. 3.

where  $V$  and  $W$  are the real and imaginary part of the DF model potential, respectively. Note that  $N_W = 1.0$  in our original calculation without  $k_{\text{cut}}$  (black solid curve in Fig. 4) as previously mentioned. The calculated result with the use of  $N_W > 1.0$  for  $k_{\text{cut}} \leq 1.5$   $\text{fm}^{-1}$  is shown in Fig. 5, where  $N_W$  value is so chosen that the calculated cross section around  $\theta_{\text{c.m.}} = 16 - 18$  degree agrees with the experimental one. It is clear that none of the calculation with the increased absorption by the use of  $N_W > 1.0$  reproduce the angular distribution of the observed cross section over the entire angular range as long as the medium

effect at high density region is largely reduced by introducing  $k_{\text{cut}} \leq 1.5 \text{ fm}^{-1}$  in the DF model calculation. These results clearly show the importance of the proper evaluation of the medium effect in the high density region ( $k_F > 1.4\text{--}1.8 \text{ fm}^{-1}$ ) and raise a strong caution to apply the complex  $G$ -matrix interaction obtained only up to  $k_F = 1.4 \text{ fm}^{-1}$  in the analyses of heavy-ion scattering through the DF model calculations. In other words, the present result implies that the medium effect in the high density region can be probed rather sensitively through the nucleus-nucleus elastic scattering experiments.

### C. Important role of three-body forces in high-density region

Next, we focus the role of the TBF effect in the high-density region. In Refs. [14, 16], we make clear the important role of the TBF effect for the nucleus-nucleus elastic scattering. In this paper, we test the sensitivity of the TBF effect in the high-density region by the following prescription for the complex  $G$ -matrix interaction;

$$v(\mathbf{s}, \rho) = \begin{cases} \text{MPa (with TBF)} \\ \dots \text{ (if } \rho = \rho_1 + \rho_2 < \rho_{\text{rep.}} \text{)} \\ \text{ESC (w/o TBF)} \\ \dots \text{ (if } \rho = \rho_1 + \rho_2 > \rho_{\text{rep.}} \text{)} \end{cases}, \quad (14)$$

where the ESC interaction is the complex  $G$ -matrix interaction constructed only from the ESC08 interaction. Namely, the ESC interaction does not include the TBF effect. The  $\rho_{\text{rep.}}$  is the parameter. In this paper, we calculate the DF potentials with several  $k_{\text{rep.}}$  values where  $k_{\text{rep.}}$  is defined by

$$\rho_{\text{rep.}} = \frac{2}{3\pi^2} k_{\text{rep.}}^3. \quad (15)$$

Namely, we replace MPa (with TBF) by ESC (w/o TBF) when the local density  $\rho$  exceed the  $\rho_{\text{rep.}}$  value. By changing the  $k_{\text{rep.}}$  value, the TBF effect in the high-density region is investigated in the potential and observable cross section.

Figure 6 shows the real and imaginary parts of the calculated DF potential with the each prescriptions for the  $^{16}\text{O} + ^{16}\text{O}$  elastic scattering at  $E/A = 70 \text{ MeV}$ . The TBF effect is clearly seen for the complex potential, especially for the inner part of the potential. In the potential, the TBF effect is clearly seen up to  $k_F = 1.8 \text{ fm}^{-1}$ . This result indicates the importance of the TBF effect in the high density region. Here, we notice that the difference

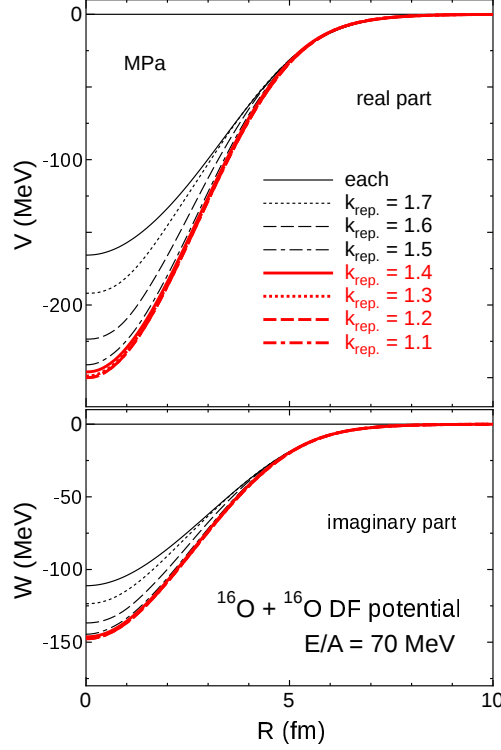


FIG. 6: (Color online) The real and imaginary parts of the DF potential in the each prescription with the  $k_{\text{rep.}}$  value. The dotted, dashed, dot-dashed, bold-solid, bold-dotted, bold-dashed, and bold-dot-dashed curves are the results with  $k_{\text{rep.}} = 1.7, 1.6, 1.5, 1.4, 1.3, 1.2$ , and  $1.1$ , respectively.

between the solid curve and  $k_{\text{rep.}} = 1.7 \text{ fm}^{-1}$  in Fig. 6 is larger than that between the solid curve and  $k_{\text{cut}} = 1.7 \text{ fm}^{-1}$  in Fig. 3. Namely, the potential with  $k_{\text{rep.}} = 1.7 \text{ fm}^{-1}$  in Fig. 6 gives deeper potential than that with  $k_{\text{cut}} = 1.7 \text{ fm}^{-1}$  in Fig. 3. This cause comes from the strength of the MPa interaction and that of the ESC interaction at  $k_{\text{rep.}} = 1.7\text{--}1.8 \text{ fm}^{-1}$ . In fact, the single-particle potential ( $U$ ) in the nuclear matter for the several cases is obtained as  $\text{Re } U_{\text{MPa}}(k_F = 1.7 \text{ fm}^{-1}) = -30.60 \text{ MeV}$ ,  $\text{Re } U_{\text{MPa}}(k_F = 1.8 \text{ fm}^{-1}) = -16.37 \text{ MeV}$ ,  $\text{Re } U_{\text{ESC}}(k_F = 1.7 \text{ fm}^{-1}) = -64.58 \text{ MeV}$ , and  $\text{Re } U_{\text{ESC}}(k_F = 1.8 \text{ fm}^{-1}) = -67.76 \text{ MeV}$ . The potential of  $k_{\text{rep.}} = 1.7 \text{ fm}^{-1}$  in Fig. 6 gives deeper potential than that of  $k_{\text{cut}} = 1.7 \text{ fm}^{-1}$  in Fig. 3 because  $\text{Re } U_{\text{ESC}}(k_F = 1.8 \text{ fm}^{-1})$  gives more attractive potential than  $\text{Re } U_{\text{MPa}}(k_F = 1.7 \text{ fm}^{-1})$ .

Figure 7 shows the results calculated with the DF potentials shown in Fig. 6 for the  $^{16}\text{O} + ^{16}\text{O}$  elastic scattering at  $E/A = 70 \text{ MeV}$ , respectively. The TBF effect is clearly seen up to  $k_F = 1.7 \text{ fm}^{-1}$  in the elastic cross section while the TBF effect up to  $k_F = 1.8 \text{ fm}^{-1}$  is

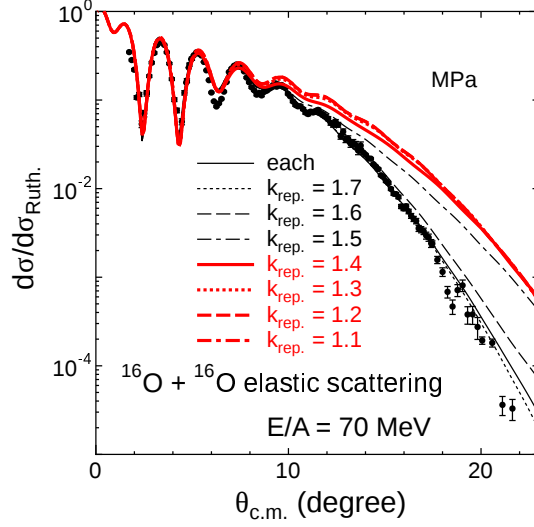


FIG. 7: (Color online) The elastic cross section with the DF potentials shown in Fig. 6. The meaning of the curves is the same as in Fig. 6.

seen in the DF potential. Here, it is first survey that the information of the medium effect in such high density region (up to  $k_F = 1.6 \text{ fm}^{-1}$ ) is extracted from the observation. In other words, this result again implies that the TBF effect in the high density region (up to  $k_F = 1.6 \text{ fm}^{-1}$ ) can be investigated from the nucleus-nucleus elastic scattering.

TABLE III: The calculated total reaction cross section for the  $^{16}\text{O} + ^{16}\text{O}$  system at  $E/A = 70$  MeV.

$k_{\text{rep.}} \text{ (fm}^{-1}\text{)}$	Total reaction cross section (mb)
1.7	1426
1.6	1426
1.5	1423
1.4	1420
1.3	1418
1.2	1416
1.1	1414

Next, we calculate the total reaction cross section with the DF potentials shown in Fig. 6. The calculated results are shown in Table III. The total reaction cross section almost has no sensitivity of the TBF effect in the high density region. Namely, it is difficult to discuss

the detail of the TBF effect in the high-density region for the total reaction cross section.

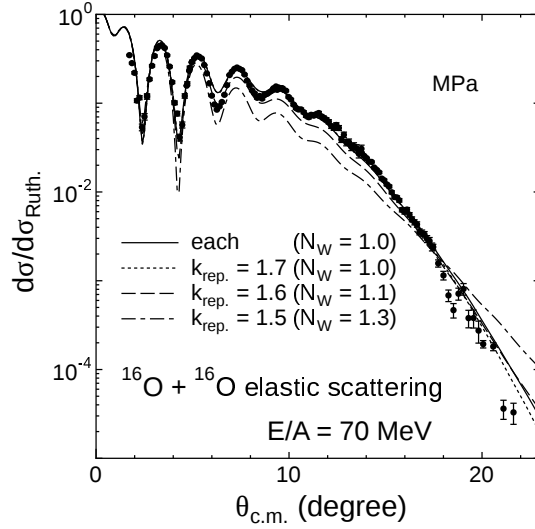


FIG. 8: The elastic cross section with the DF potentials shown in Fig. 6 in the case with the renormalization factor,  $N_W$ , for the imaginary part. The meaning of the curves is the same as in Fig. 6.

Here, we also test the effect of the renormalization factor for the imaginary part of the DF potential. The calculated result is shown in Fig. 8. We set the renormalization factor to reproduce the data around  $16\text{--}18^\circ$ . However, the elastic cross sections calculated with  $k_{\text{rep.}} = 1.6 \text{ fm}^{-1}$  and  $k_{\text{rep.}} = 1.5 \text{ fm}^{-1}$  can not reproduce the data around  $6\text{--}16^\circ$ . The important role of the TBF effect in the high-density region is confirmed in the nucleus-nucleus elastic cross section. This result again implies that the nucleus-nucleus elastic scattering can sensitively probe the important role of the TBF effect in the high density region up to  $k_F = 1.6 \text{ fm}^{-1}$ .

#### IV. SUMMARY AND REMARKS

In summary, we have constructed the DF potential with the complex  $G$ -matrix interaction including the TBF effect based on the MPP model. With the DF potential, we first investigate the sensitivity of the evaluating position of the local density. The evaluating position has a minor role to the potential and cross section for the  $^{16}\text{O} + ^{16}\text{O}$  system. The effect of the evaluating position might be seen with smaller nucleus than the  $^{16}\text{O}$  nucleus

but it is the future issue. Second, the medium effect in the high-density region have been investigated by cutting the local density in the high density region. The medium effect is clearly seen in the potential and the elastic scattering cross section, but not in the total cross section. In addition, the TBF effect in the high-density region have also been investigated. The TBF effect up to  $k_F = 1.6 \text{ fm}^{-1}$  has a critical role to determine the elastic angular distribution. Here, we should mention that similar results are obtained with the use of the CEG07 or MPb/c interactions [15, 19] instead of the MPa one adopted here. These results imply that the medium effect, especially the TBF effect, in the high-density region can be probed by the observed nucleus-nucleus elastic scattering. Namely, the observed nucleus-nucleus elastic scattering gives us a fruitful information on the EOS of high density nuclear matter. In addition, we have raised a caution in the use of the  $G$ -matrix interactions evaluated only up to the normal density, such as the JLM, the original CEG and Melbourne interactions, to the analyses of nucleus-nucleus scattering/reactions through the DF model framework. Finally, we made clear the crucial role of the TBF effect in the high-density region on the nucleus-nucleus elastic scattering.

## V. ACKNOWLEDGMENT

The authors acknowledge Professor Uesaka for encouraging comments.

- 
- [1] G. Bertsch, J. Borysowicz, H. McManaus, and W. G. Love, Nucl. Phys. **A284**, 399 (1977).
  - [2] G. R. Satchler and W. G. Love, Phys. Rep. **55**, 184 (1979).
  - [3] A. M. Kobos, B. A. Brown, P. E. Hodgson, G. R. Satchler, and A. Budzanowski, Nucl. Phys. **A384**, 65 (1982).
  - [4] M. E.-A. Farid and G. R. Satchler, Nucl. Phys. **A438**, 525 (1985).
  - [5] D. T. Khoa, W. von Oertzen, and H. G. Bohlen, Phys. Rev. C **49**, 1652 (1994).
  - [6] M. E. Brandan and G. R. Satchler, Phys. Rep. **285**, 143 (1997).
  - [7] D. T. Khoa, G. R. Satchler, and W. von Oertzen, Phys. Rev. C **56**, 954 (1997).
  - [8] S. Nagata, M. Kamimura, and N. Yamaguchi, Prog. Theor. Phys. **73**, 512 (1985).
  - [9] F. Carstoiu and M. Lassau, Nucl. Phys. **A597**, 269 (1996).



- [10] L. Trache, A. Azhari, H. L. Clark, C. A. Gagliardi, Y.-W. Lui, A. M. Mukhamedzhanov, R. E. Tribble, and F. Carstoiu, Phys. Rev. C **61**, 024612 (2000).
- [11] J. C. Blackmon, F. Carstoiu, L. Trache, D. W. Bardayan, C. R. Brune, C. A. Gagliardi, U. Greife, C. J. Gross, C. C. Jewett, R. L. Kozub, et al., Phys. Rev. C **72**, 034606 (2005).
- [12] T. Furumoto and Y. Sakuragi, Phys. Rev. C **74**, 034606 (2006).
- [13] D. T. Khoa, W. von Oertzen, H. G. Bohlen, and S. Ohkubo, J. Phys. G: Nucl. Part. Phys. **34**, R111 (2007).
- [14] T. Furumoto, Y. Sakuragi, and Y. Yamamoto, Phys. Rev. C **80**, 044614 (2009).
- [15] T. Furumoto, Y. Sakuragi, and Y. Yamamoto, Phys. Rev. C **78**, 044610 (2008).
- [16] T. Furumoto, Y. Sakuragi, and Y. Yamamoto, Phys. Rev. C **79**, 011601(R) (2009).
- [17] T. Furumoto, W. Horiuchi, M. Takashina, Y. Yamamoto, and Y. Sakuragi, Phys. Rev. C **85**, 044607 (2012).
- [18] Y. Yamamoto, T. Furumoto, N. Yasutake, and T. A. Rijken, Phys. Rev. C **88**, 022801(R) (2013).
- [19] Y. Yamamoto, T. Furumoto, N. Yasutake, and T. A. Rijken, arXiv:1406.4332.
- [20] T. A. Rijken, M. M. Nagels, and Y. Yamamoto, Prog. Theor. Phys. Suppl. **185**, 14 (2010).
- [21] T. A. Rijken, M. M. Nagels, and Y. Yamamoto, Genshikaku Kenkyu **57 Suppl. 3**, 6 (2013), proceedings of the International Workshop on Strangeness Nuclear Physics, 2012.
- [22] B. Sinha, Phys. Rep. **20**, 1 (1975).
- [23] B. Sinha and S. A. Moszkowski, Phys. Rev. **B81**, 289 (1979).
- [24] J. W. Negele and D. M. Vautherin, Phys. Rev. C **5**, 1472 (1972).
- [25] X. Campi and A. Bouyssy, Phys. Lett. B **73**, 263 (1978).
- [26] D. T. Khoa, Phys. Rev. C **63**, 034007 (2001).
- [27] F. A. Brieva and J. R. Rook, Nucl. Phys. A **291**, 299 (1977).
- [28] F. A. Brieva and J. R. Rook, Nucl. Phys. A **291**, 317 (1977).
- [29] F. A. Brieva and J. R. Rook, Nucl. Phys. A **297**, 206 (1978).
- [30] N. Yamaguchi, S. Nagata, and T. Matsuda, Prog. Theor. Phys. **70**, 459 (1983).
- [31] K. Minomo, K. Ogata, M. Kohno, Y. R. Shimizu, and M. Yahiro, J. Phys. G: Nucl. Part. Phys. **37**, 085011 (2010).
- [32] M. Katsuma, Y. Sakuragi, S. Okabe, and Y. Kondo, Prog. Theor. Phys. **107**, 377 (2002).
- [33] S. Okabe, in *Tours Symposium on Nuclear Physics II*, edited by H. Utsunomiya, M. Ohta,

- J. Galin, and G. Mhnzenberg (World Scientific, Singapore, 1995), p. 112.
- [34] F. Nuoffer, G. Bartnitzky, H. Clement, A. Blazevic, H. G. Bohlen, B. Gebauer, W. von Oertzen, M. Wilpert, T. Wilpert, A. Lepine-Szily, et al., *Nuovo Cimento A* **111**, 971 (1998).
- [35] J. P. Jeukenne, A. Lejeune, and C. Mahaux, *Phys. Rev. C* **16**, 80 (1977).
- [36] N. Yamaguchi, S. Nagata, and J. Michiyama, *Prog. Theor. Phys.* **76**, 1289 (1986).
- [37] K. Amos, P. J. Dortmans, H. V. von Geramb, and S. Karataglidis, *Adv. Nucl. Phys.* **25**, 275 (2000).